JOURNAL OF CATALYSIS **159,** 162–169 (1996)
ARTICLE NO. 0075

Silver-Cluster Formation on $AgZr_2(PO_4)_3$ and Catalytic Decomposition of Butan-2-ol

Saïd Arsalane,* Mahfoud Ziyad,*,[1] Gisèle Coudurier,† and Jacques C. Védrine†

*Laboratoire de Physico-Chimie des Matériaux et Catalyse, Faculté des Sciences, Rabat, Morocco; and †Institut de Recherches sur la Catalyse (CNRS), 2 Avenue Albert Einstein, F-69626 Villeurbanne, France

Received December 1, 1994; revised October 16, 1995; accepted October 31, 1995

A Nasicon-type $AgZr_2(PO_4)_3$ material was synthesized and its catalytic properties were characterized by butan-2-ol conversion in the presence and absence of oxygen. The catalytic activity was mainly oriented toward the production of methyl ethyl ketone and butenes. Activity was shown to depend on the reducibility of the Ag^+ ions and on the oxygen concentration in the reactants. Hydrogen, butan-2-ol, and butan-2-ol/O_2 were able to reduce the Ag^+ cations located in the three-dimensional channels of the phosphate network. Silver clusters appeared on the surface and protons replaced the Ag^+ ions in the structure to form (HPO_4) acidic groups, without any modification in the framework of the phosphate. Evidence for this phenomenon was provided by (i) XRD peaks corresponding to (111) and (200) metallic silver diffractions, (ii) UV–visible spectroscopy which showed conduction bands at 372 and 410 nm attributed to Ag^0 crystallites and a shoulder in the 250–270 nm region due probably to $(Ag_n)^{\delta+}$ charged clusters, (iii) TEM analysis which revealed that the exposure of the phosphate to the electron beam produced a spontaneous appearance of silver particles, (iv) IR spectroscopy which demonstrated the protonation of the sample by the appearance of three new hydroxyl bands in the 3000–3500 cm^{-1} region, a result supported by ^1H NMR spectroscopy, and (v) TPO experiments performed after the reduction of the sample which showed that silver clusters adsorb oxygen in at least two specific ways which are active in the oxidative dehydrogenation of the butan-2-ol. It was also shown that the formation of silver particles was reversible upon reoxidation at 773 K to give the starting material $AgZr_2(PO_4)_3$.

INTRODUCTION

Nasicon-type phosphates of general formula $M_xM'_y(PO_4)_3$ constitute a wide family of compounds extensively studied for their numerous properties such as ionic conductivity (1), ion exchange capacity (2), low thermal expansion coefficients (3), and catalytic activity (4).

The structure of $AgZr_2(PO_4)_3$ was at first established by Hagman (5). It can be described as a three-dimensional network containing ($M'O_6$) octahedra and (PO_4) tetrahedra sharing corners and developing interconnected cavities. Silver ions located in the channels have an ionic mobility similar to that found for β-alumina (6).

Recently, the catalytic activities of $Cu_n(Ti, Zr)_2(PO_4)_3$ in alcohol decomposition (7, 8) and propylene oxidation have been investigated (9, 10). The activities were correlated with the reduction of the mobile ions and with the properties of the metallic particles generated *in situ* on the surface of the phosphate. This reduction and perhaps also the mobility of the cations in the channels depend on the synthesis route and on the thermal history of the phosphate. It was found that $Ag_2ZrSc(PO_4)_3$ under particular conditions may have an oscillatory activity in the oxidation of C_3H_6 (11). This striking behavior was attributed to the ability of silver to undergo surface oxido-reduction processes involving a Mars and van Krevelen mechanism (12).

The present work is an extension of the investigations carried out on $AgZr_2(PO_4)_3$ Nasicon-type phosphate in propylene oxidation (13), which showed that acrolein production depends strongly on the amount of Ag^+ ions reduced *in situ* and on the composition of the reactants. An increase in the oxygen relative concentration enhances the total oxidation of C_3H_6 and decreases the acrolein production. A right choice of oxygen to propylene ratio $[O_2]/[C_3H_6]$ synchronizes the parameters governing the oscillatory phenomenon and gives rise to activity and temperature oscillations. Similar behavior was observed on nonsupported polycrystalline silver (13).

In order to gain new insight into the main features of silver contained in nonconventional catalysts, an investigation of the behavior of $AgZr_2(PO_4)_3$ was carried out in the butan-2-ol decomposition reaction. The choice of this reaction was justified by the high reactivity of this alcohol and because it provides useful information about (i) the acido-basic properties of the catalyst, (ii) the redox properties of the active centers, and (iii) in this particular case the *in situ* reduction of Ag^+ ions to metallic silver during the reaction.

[1] To whom correspondence should be addressed.

0021-9517/96 $18.00

EXPERIMENTAL

Catalyst Preparation

The $AgZr_2(PO_4)_3$ sample employed in the present investigation was prepared by coprecipitation as previously described (10). Stoichiometric quantities of $ZrOCl_2 \cdot 8H_2O$, $AgNO_3$, and $(NH_4)_2HPO_4$ (Merck products) were dissolved in a minimal amount of water under stirring at room temperature. The amorphous precipitate obtained was heated to 343 K and maintained at that temperature until all the water had evaporated. The solid recovered was submitted to cycles of grinding and heating to 773 K. The resulting material was then calcined in air at 1173 K for 48 h. Its chemical composition was determined by atomic absorption and was found to correspond to the stoichiometry of silver–zirconium phosphate $AgZr_2(PO_4)_3$.

Catalyst Characterization

The sample was characterized before and after the catalytic runs by several physical techniques in order to correlate its activity with the transformations it might have undergone under reaction conditions. X-ray diffraction patterns were recorded with a Philips PW 1710 diffractometer using Cu$K\alpha$ radiation.

FTIR spectra were obtained with a Bruker/IFS 48 spectrometer. The sample was suspended in ethanol, sprayed on a CaF_2 disk, and introduced into the IR cell. This cell permitted *in situ* and static experiments. It could be evacuated at a given temperature or filled with a chosen atmosphere.

Diffuse reflectance spectra were recorded in the 200–700 nm range on a Perkin Elmer (Lambda 9) spectrometer equipped with an integrating sphere. $BaSO_4$ was used as a reference.

^{31}P and ^{1}H NMR spectra were recorded at room temperature with a Bruker CXP 300 spectrometer equipped with a magic angle spinning accessory. The chemical shifts were measured using as references H_3PO_4 for ^{31}P and H_2O for ^{1}H.

Electron micrographs for $AgZr_2(PO_4)_3$ were obtained using a high resolution (ca. 0.2 nm) JEOL JEM 100CX transmission electron microscope.

Temperature Programmed Oxidation

The temperature programmed oxidation (TPO) experiments were carried out in the conventional apparatus described elsewhere (14). The catalyst sample ($m = 0.200$ g), in powder form, was placed in a quartz microreactor and reduced by exposing it for 1 h to a flow of hydrogen at 623 K. After this reduction the sample was submitted to TPO using 5 vol% O_2 in He at a total flow rate of 25 cm^3 min^{-1} and a heating rate of 10 K min^{-1} up to 873 K.

Catalytic Measurements

Catalytic activity of $AgZr_2(PO_4)_3$ was investigated in butan-2-ol decomposition. This probe reaction allows the characterization of the acido-basic properties of the solid as well as its redox behavior in the oxidative dehydrogenation of the alcohol. It also offers the advantage to follow qualitatively the silver migration toward the surface of the phosphate by the concomitant changes that the catalytic reaction induces on the activity.

Activity measurements were performed in a U-shaped quartz continuous microreactor operated at atmospheric pressure. Prior to each rum, 0.100 g of the catalyst ground and sieved in particles with size ranging between 110 and 125 μm were pretreated under a 60 cm^3 min^{-1} flow of nitrogen at 723 K for 2 h. The alcohol diluted in N_2 or air was supplied to the reactor at a constant pressure (8.3×10^2 Pa) by a saturator held at 283 K. The total flow rate of the carrier gas and the reactants was kept at 60 cm^3 min^{-1}. Quantitative analysis of the reaction mixture was undertaken by gas chromatography (FID) on a 4-m (1/8 in.) stainless-steel column packed with Carbowax 1500 (15%) on chromosorb PAW (60/80 mesh). Carbon dioxide was analyzed by a second chromatograph equipped with catharometers and a 2-m (1/8 in.) stainless-steel column containing Porapack Q.

RESULTS AND DISCUSSION

Characterization of $AgZr_2(PO_4)_3$ before and after Reduction

X-ray diffraction analysis of the sample as synthesized (Fig. 1a) showed that the phosphate is a pure phase belonging to the rhombohedral system $R\bar{3}c$. Its three-dimensional structure is made up of zeolitic-type channels containing cavities occupied by silver. The unit cell parameters are reported in Table 1. The calculated dimensions are consistent with the results reported for the related structures $NaZr_2(PO_4)_3$ and $AgTi_2(PO_4)_3$.

^{31}P MAS NMR spectra of the sample (Fig. 2) recorded at room temperature showed only one sharp and narrow resonance with a chemical shift $\delta = -24.4$ ppm as in the case of $NaZr_2(PO_4)_3$ (15). It can be concluded that no difference in phosphorus atom positions was detected, in agreement with

TABLE 1

Unit Cell Parameters

Phosphate	a (nm)	b (nm)	V (nm^3)
$NaZr_2(PO_4)_3$	0.884	2.275	1.540
$AgZr_2(PO_4)_3$	0.883	2.292	1.548
$AgTi_2(PO_4)_3$	0.847	2.211	1.374

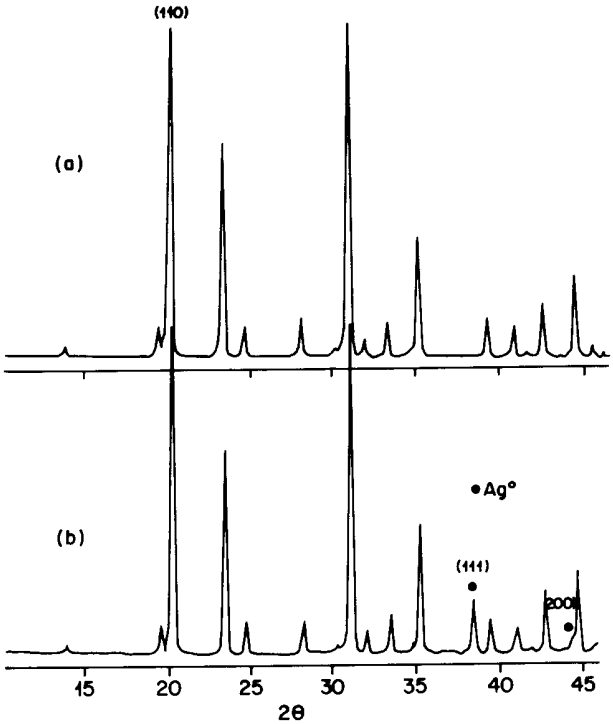

FIG. 1. XRD of $AgZr_2(PO_4)_3$ (a) before the catalytic test or after the TPO run and (b) after the catalytic test in the absence of oxygen.

the space group $R\bar{3}c$ in which all P atoms occupy equivalent crystallographic positions.

The UV–visible absorption spectrum of $AgZr_2(PO_4)_3$ is given in Fig. 3a. It shows only two bands appearing in the charge transfer domain. The first one located at 232 nm and assigned to the electronic transfer $O^{2-} \rightarrow Zr^{4+}$ is usually observed in zirconium Nasicon-type phosphates (16). The second one centered at 210 nm may be attributed to the

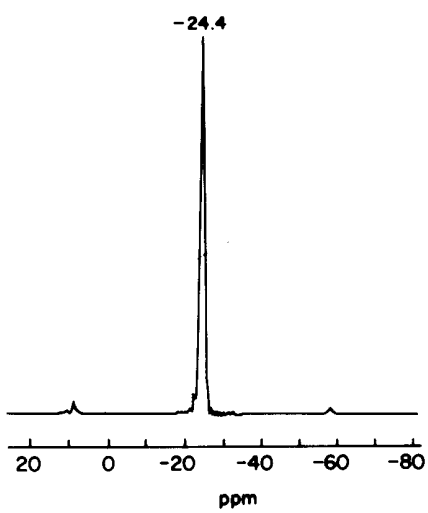

FIG. 2. ^{31}P MAS NMR spectra of $AgZr_2(PO_4)_3$.

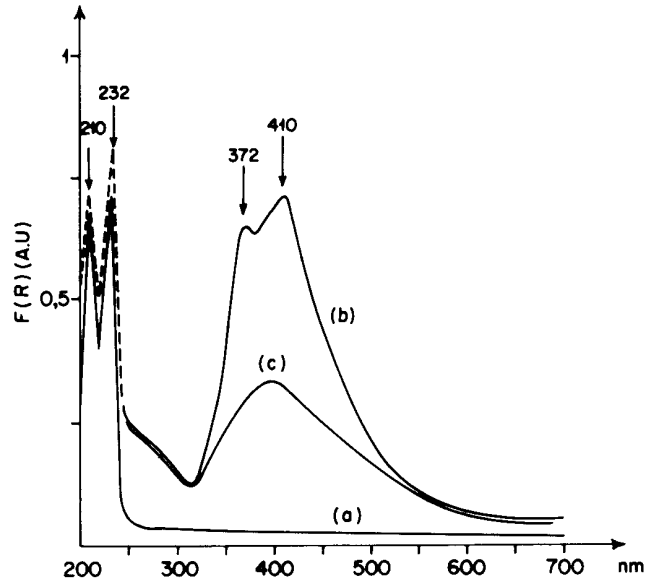

FIG. 3. UV–visible reflectance spectra of $AgZr_2(PO_4)_3$ (a) before the catalytic test, (b) after contacting with butan-2-ol, and (c) after the catalytic test in the presence of oxygen at 493 K.

electronic transitions of Ag^+ ions between ^1S ($4d^{10}$) and ^3D ($4d^9\,5s^1$) states. Charge transfers between O^{2-} and Ag^+ might also exist in this region (17).

The reduction of Ag^+ ions in the phosphate was carried out at various temperatures with a flowing stream of H_2 at atmospheric pressure (10). The process was found to be exothermic with a subsequent appearance of metallic silver particles on the material as evidenced by XRD reflections at $2\theta = 38°30'$ and $44°40'$ which correspond, respectively, to Ag (111) and (200) planes. There were no changes in the phosphate XRD pattern (Fig. 1b) except for a slight shift of the diffraction peaks toward larger 2θ values assigned to a slight contraction of the unit cell.

The amounts of metallic silver obtained at various temperatures were calculated from the intensity ratios of the (111) reflection of silver and the (110) reflection of the phosphate. The values reported in Table 2 show that the reduction level increases with the temperature of reduction.

TEM observations to $AgZr_2(PO_4)_3$ showed that a few seconds exposure of the sample to the electron beam produces spontaneously the appearance of metallic silver particles on the surface. Figure 4 shows typical micrographs taken after the massive changes in the sample were over. Silver particles formed have a globular shape which is believed

TABLE 2

Percentage Reduction of Ag^+ by H_2 vs Temperature

Temperature (K)	473	673	773	823	973
$I_{Ag}/I_{Phosphate}100$	5	10	20	30	40

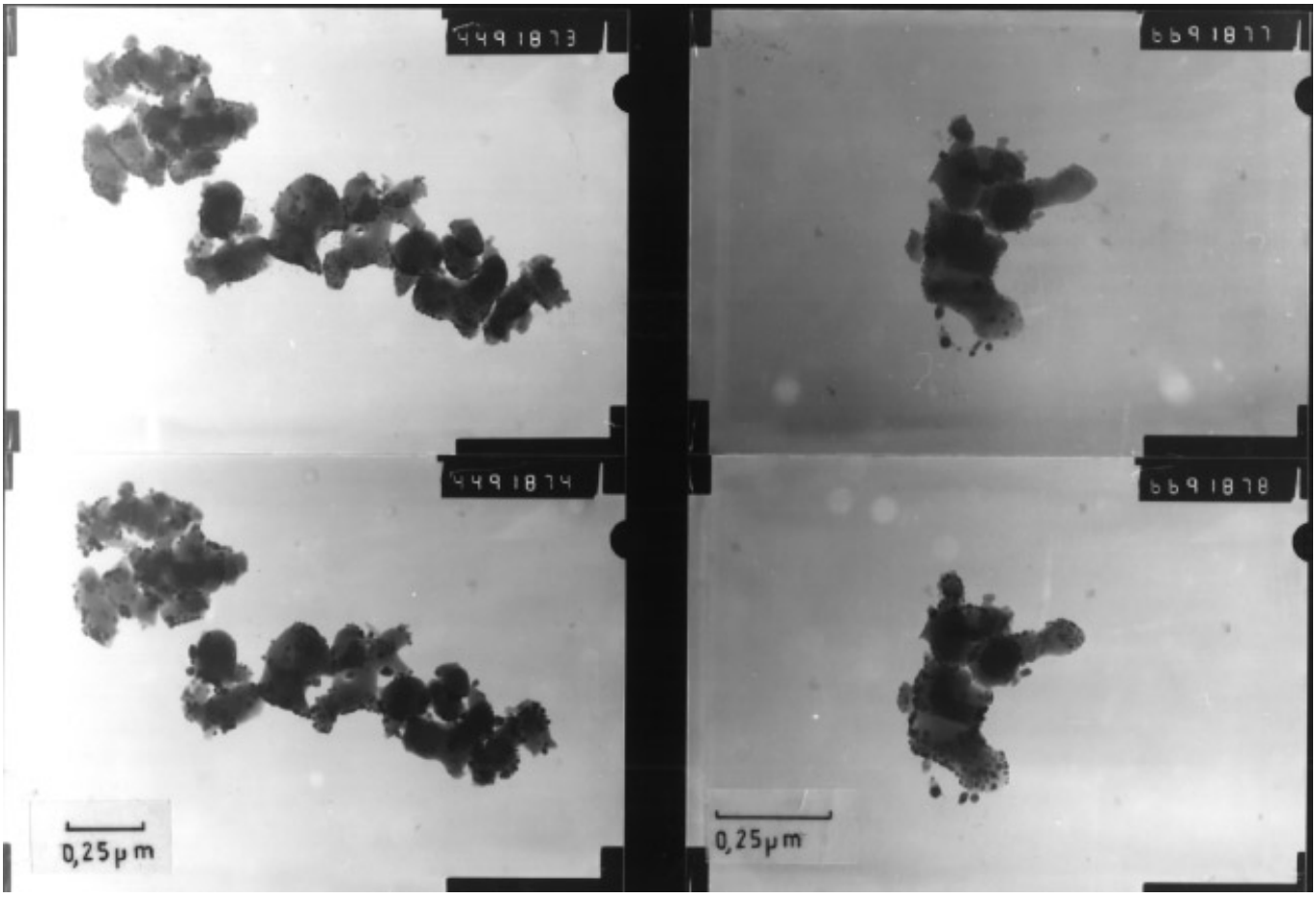

FIG. 4. TEM micrographs of $AgZr_2(PO_4)_3$.

to be indicative of a weak metal–support interaction. Their distribution is relatively homogenous and their size ranges predominantly between 10 and 30 nm. A similar reduction phenomenon was observed with $AgTi_2(PO_4)_3$ (18). It can be explained by the high mobility of Ag^+ ions which migrate out of the channels of the phosphate network and are reduced by the electron beam.

The IR spectrum (Fig. 5) of $AgZr_2(PO_4)_3$ treated *in situ* by H_2 at 623 K for 1 h shows three absorption bands at 3490, 3270, and 3165 cm^{-1} assignable to the vibrations ν_{OH} of $[PO_3OH]$ groups (19). No water was observed to form as shown by the absence of bands around 1600 cm^{-1}.

^1H MAS NMR investigations also confirmed the appearance of new hydroxyl groups, as shown in Figs. 6a and 6b where the spectra were recorded before and after reduction. A comparison of the two spectra shows the presence of new resonances with chemical shifts at $\delta = -1.8$, $\delta = 0.6$, and $\delta = 7.0$ ppm which may be attributed to protons located in the channels of the phosphate network.

All these results indicate that upon reduction Ag^+ ions in the structure migrate to the surface where they form metallic silver particles and that this nucleation is accompanied by the protonation of the sample. The mechanism of the silver nucleation is supposedly similar to that described by Cheng and Clearfield for $Ag_2Zr(PO_4)_2$ (20) and can be expressed as

$$AgZr_2(PO_4)_3 + x/2\,H_2 \rightarrow Ag_{1-x}H_xZr_2(PO_4)_3 + xAg^0. \quad [1]$$

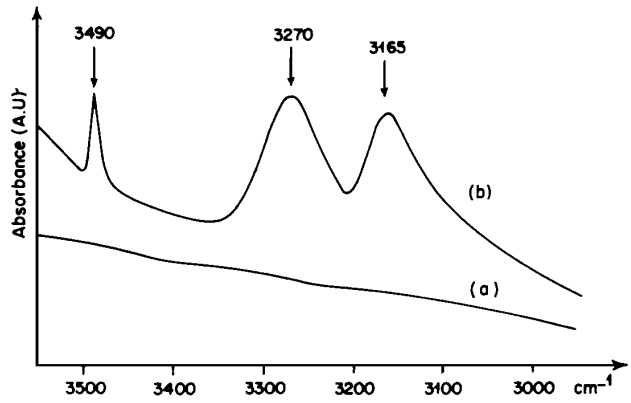

FIG. 5. FTIR spectra of (a) $AgZr_2(PO_4)_3$, (b) $xAg^0/Ag_{1-x}H_xZr_2(PO_4)_3$.

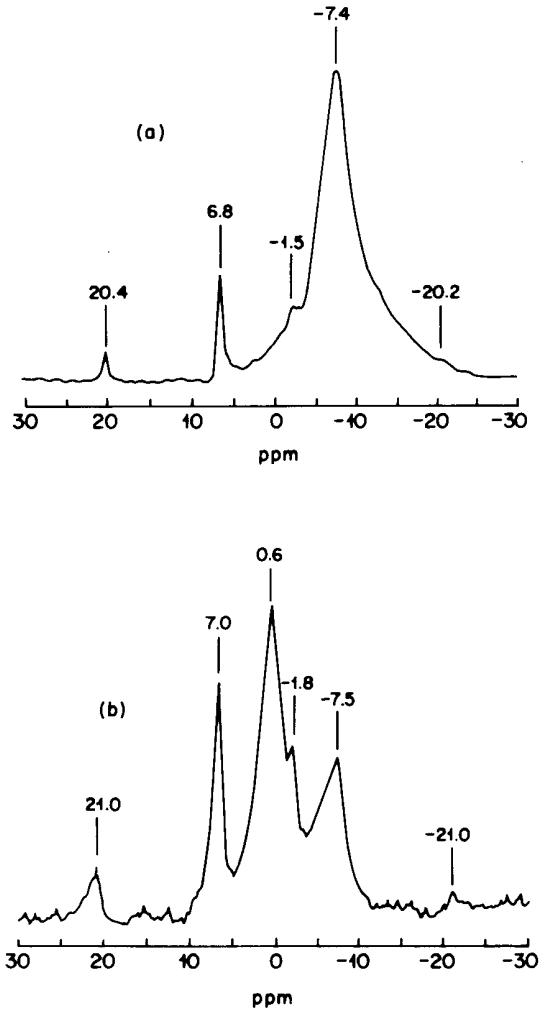

FIG. 6. ^{1}H MAS NMR spectra of $AgZr_2(PO_4)_3$ (a) before reduction, and (b) after reduction by H_2 at 623 K.

The reduction of Ag^+ ions and their subsequent replacement by protons does not affect the structure of the phosphate. However, the slight shift of the diffraction peaks in the XRD patterns toward larger angles due to the difference between the ionic radius of Ag^+ and H^+ ions provides evidence for the substitution of Ag^+ ions by protons.

An oxidation of the prereduced sample with H_2 for 1 h at 623 K was carried out employing the temperature programmed oxidation technique. A typical TPO profile is reported in Fig. 7. It shows, two overlapping peaks corresponding presumably to two distinct processes. The first peak centered at 573 K may be attributed as shown by its broad form to a progressive adsorption of O_2 on Ag particles. This adsorption takes place as reported in the literature on different sites giving distinct oxygen species (21, 22). The associated reaction may be formulated as

$$Ag_{1-x}H_xZr_2(PO_4)_3 + xAg^0 + y/2\,O_2 \rightarrow Ag_{1-x}H_xZr_2(PO_4)_3 + Ag_x\text{–}O_y, \quad [2]$$

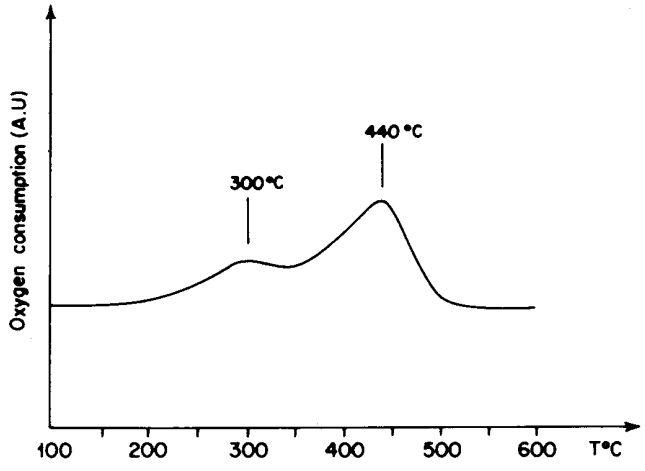

FIG. 7. Temperature programmed oxidation (TPO) profile of $AgZr_2(PO_4)_3$ reduced at 623 K for 1 h. O_2 (5 vol%) in He. Total flow rate = 25 cm^3 min^{-1}. Heating rate = 10 K min^{-1}.

where Ag_x–O_y stands for various kinds of adsorbed oxygen on silver crystallites. Oxygen uptake computed from the area of the peak was 5.81×10^{-3} mol of oxygen per mol of the phosphate.

The second oxygen consumption was quantitatively more important than the first. It reaches its maximum at 713 K and extends up to 773 K. It can be associated with at least two processes, namely the migration of Ag^+ ions back into the phosphate lattice and the concomitant production of water detected in the outlet gases by hygrometer. The overall reaction may then be written:

$$Ag_{1-x}H_xZr_2(PO_4)_3 + Ag_x\text{–}O_y + (x/4 - y/2)\,O_2 \rightarrow AgZr_2(PO_4)_3 + xH_2O. \quad [3]$$

Oxygen uptake corresponding to this second peak was found to be 1.55×10^{-2} mol of oxygen per mol of the phosphate. The total amount consumed during the TPO run is then equal to 2.13×10^{-2} or $x/4$ mol of O_2 per mol of the phosphate, as indicated by Eq. [3]. Therefore, assuming that the oxidation of silver by O_2 gave mainly Ag_x–O_y species, the percentage of Ag° dispersed on the surface by H_2 reduction at 623 K was calculated to be 8.5%. This quantity is in good agreement with the results reported in Table 2.

Evidence for silver retrodiffusion in the phosphate lattice at the end of the TPO run was provided by X-ray diffraction analysis and UV–visible spectroscopy. They indicate that the starting material $AgZr_2(PO_4)_3$ is recovered (Fig. 1a and Fig. 3a). Furthermore, XPS analysis of the sample after the TPO showed that the stoichiometry of the surface was as in $AgZr_2(PO_4)_3$. Similar results were reported on zeolites exchanged with silver (23).

Catalytic Properties

The catalytic activity of $AgZr_2(PO_4)_3$ was measured on a sample with a surface area of 3 m^2 g^{-1}. Figure 8 reports

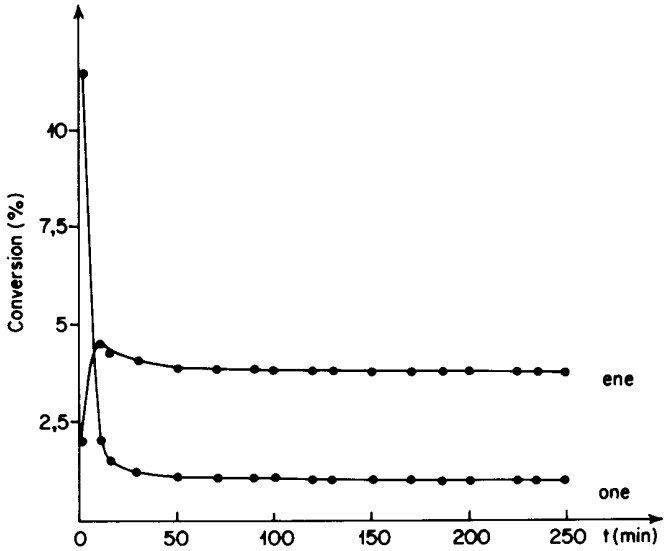

FIG. 8. Butan-2-ol conversion in butene (α_{ene}) and methyl ethyl ketone (α_{one}) over 0.100 g for $AgZr_2(PO_4)_3$ at 493 K in the absence of O_2. ($P_{alcohol} = 8.3 \times 10^2$ Pa. Total flow rate = 60 cm^3 min^{-1}).

the alcohol conversion into butenes (α_{ene}) and methyl ethyl ketone (α_{one}) at 493 K using a reactant mixture free of oxygen. Methyl ethyl ketone production drops abruptly during the first 10 min of reaction to reach a steady state where the conversion level does not exceed 1%. At the same time the dehydration activity increases and stabilizes after 2 h at 3.75%. Introduction of various concentrations of oxygen into the reaction mixture deeply modifies the catalyst behavior. Figure 9 reports the conversions into butenes, CO_2, and methyl ethyl ketone versus time at different O_2 vol%. Globally the dehydrogenation activity increases. An enrichment in O_2 of the reaction mixture enhances the dehydrogenation activity and the total oxidation (α_{CO_2}). The dehydration activity decreases slightly. Figure 10 displays the results obtained at steady state and shows that α_{one} increases linearly with the increase of oxygen concentration in the carrier gas. During the first half hour of the reaction both activities are characterized by transitory behavior which is probably due to modifications of the catalyst surface under the reactants. In the special case of the dehydrogenation one can visualize on the corresponding curves (Fig. 9) the previously mentioned redox processes. During the first minutes the activity decreases. This drop can be associated with the reduction of Ag^+ ions and their migration toward the surface. The increasing part of the curves can be related to the oxidation of the silver particles which constitute the active species in the oxidative dehydrogenation.

Similar Nasicon-type phosphates such as $Cu_n(Ti, Zr)_2(PO_4)_3$ have been investigated in the same probe reaction. Titanium materials were found to be less active than those containing zirconium, presumably because the ionic radius of Ti^{4+} ($r_{Ti}^{4+} = 0.061$ nm) is smaller than that of Zr^{4+} ($r_{Zr}^{4+} = 0.072$ nm). Consequently, the conduction channels

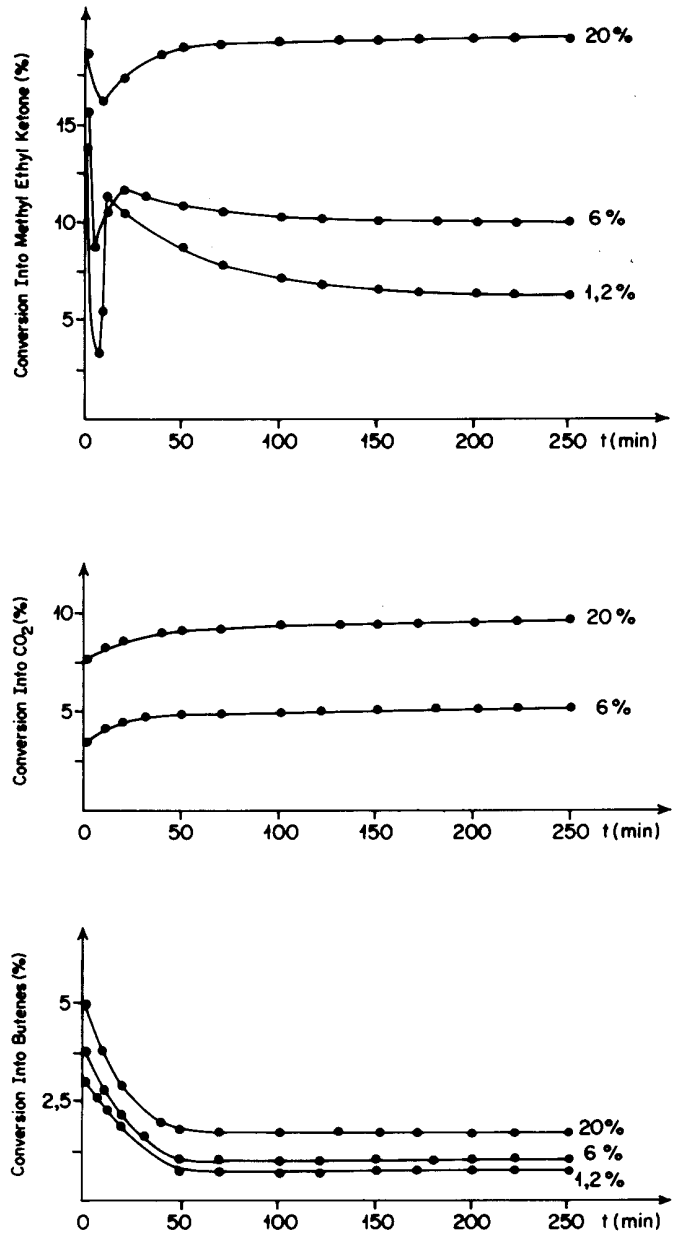

FIG. 9. Butan-2-ol conversion over $AgZr_2(PO_4)_3$ at 493 K in the presence of different percentages by volume of O_2 in the reaction mixture. ($P_{alcohol} = 8.3 \times 10^2$ Pa. Total flow rate = 60 cm^3 min^{-1}).

in (Ag, Cu) $Ti_2(PO_4)_3$ are narrower and the diffusion process of the active cations (Ag^+ or Cu^+) toward the surface requires more energy. The difference between the Zr^{4+} and Ti^{4+} electronegativities and therefore the polarizability of the channels does not intervene in the catalytic behavior. The only factor that influences the activity, as shown by experimental data, is the tunnel size (10).

Characterization after Catalysis

XRD patterns (Fig. 1b) of the sample recorded after a catalytic test carried out in an atmosphere free of oxygen

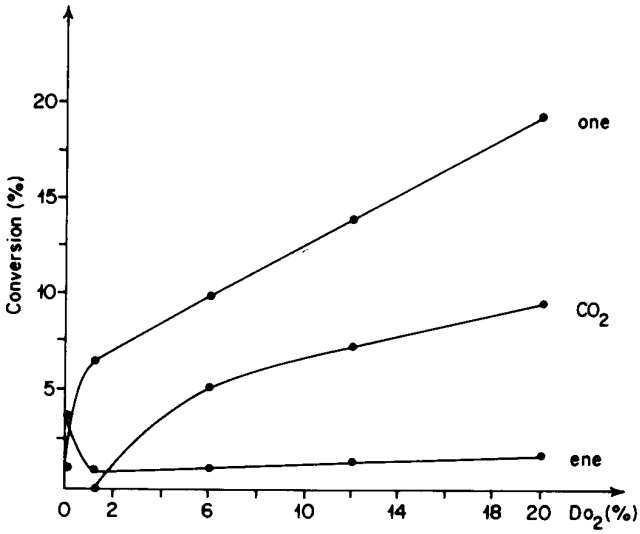

FIG. 10. Butan-2-ol conversion into butene CO_2 and methyl ethyl ketone vs percentage of O_2 by volume in the reactants.

show the appearance of the two reflections at $2\theta = 38°30'$ and $44°40'$ belonging, respectively, to silver (111) and (200) planes. Likewise the color of the sample changed from white to greyish. UV–visible spectra of the sample after a catalytic run (Fig. 3b) show two new bands centered at 372 and 410 nm and a shoulder in the 250–270 nm region. The two bands (410 and 372 nm) are attributed to silver crystallites of different sizes, previously identified by TEM analysis as shown in Fig. 4. The weak band located at 250–270 nm might be associated as reported in the literature with the formation of linear $(Ag_n)^{\delta+}$ charged clusters by an activated process.

The treatment of $AgZr_2(PO_4)_3$, either by H_2 or butan-2-ol, resulted in the formation of Ag^0 particles and protonation of the sample. In the absence of oxygen the silver that migrated during the reaction is not very active in the dehydrogenation, while the exchanged protons enhance the dehydration activity (Fig. 8). Butan-2-ol, as shown, reduces the sample. The involved reaction can be written as in the similar case of $CuZr_2(PO_4)_3$ (24):

$$AgZr_2(PO_4)_3 \xrightarrow{\text{[butan-2-ol]}} Ag_{1-x}H_xZr_2(PO_4)_3 + xAg^0. \quad [4]$$

When the reaction is carried out in the presence of a gaseous mixture containing oxygen the catalyst performance improves. A production of carbon dioxide appears, too. At steady state, in the presence of a feed containing 20 vol% O_2, dehydrogenation activity becomes 20 times more important. This enhancement of the activity is attributed to the oxidative dehydrogenation of the butan-2-ol on Ag^0 crystallites which appear on the surface of the phosphate. As a matter of fact, TPO experiments have shown that silver adsorbs oxygen giving rise to Ag_x–O_y species which act as the active sites in the alcohol dehydrogenation and combustion.

It was observed (Fig. 10) that an enrichment of the reaction mixture with O_2 increases carbon dioxide production. As suggested in the literature, this effect may be related to specific adsorbed oxygen on silver (25, 26).

The dehydration activity in the presence of O_2 in the reactants decreases to reach less than 2% at steady state. This decrease may be attributed to the opposite partial exchange H^+–Ag^+ which produces water. The reaction may be written as

$$xAg^0 + Ag_{1-x}H_xZr_2(PO_4)_3 \xrightarrow{[xO_2]} AgZr_2(PO_4)_3 + x/2\,H_2O. \quad [5]$$

Obviously this exchange is limited to the acidic protons which are on the surface of the sample; those located "inside" the phosphate are not accessible to the reactants.

CONCLUSIONS

The catalytic properties of silver–zirconium phosphate $AgZr_2(PO_4)_3$ are related, as shown by all the results, to its structural characteristics:

(i) Ag^+ ions may be easily reduced to metallic silver and perhaps charged clusters either by hydrogen or butan-2-ol under reaction conditions.

(ii) The silver ions are replaced in the lattice of the phosphate by protons which create acidic sites [P–OH] active in the dehydration reaction.

(iii) The small silver particles (10–30 nm) generated *in situ* are active in the oxidative dehydrogenation of butan-2-ol. TPO results showed that the silver-loaded $Ag_{1-x}H_xZr_2(PO_4)_3$ adsorbs different forms of oxygen. The obtained silver particles seemed to display properties characteristic of bulk metal. The mechanism involved in alcohol oxidation was suggested to be of the Mars and van Krevelen type.

(iv) Under oxygen (air) at moderate temperatures (773 K) the silver crystallites and the clusters diffuse back into the lattice restoring the initial material $AgZr_2(PO_4)_3$. The phosphate structure was not altered by this redox process.

ACKNOWLEDGMENTS

The authors thank the support staff of the facilities at the I.R.C., especially Mrs. B. Jouguet for her contribution in the TPR/TPO experiments. Financial support (A.I.M. 91/567) for this work was provided by the French Embassy in Rabat.

REFERENCES

1. Goodenough, J. B., Hong, H. Y. P., and Kafalas, J., *Mater. Res. Bull.* **11**, 203 (1976).
2. Nadiri, A., and Delmas, C., *C. R. Acad. Sci. Paris* **304**, 9 (1987).
3. Alamo, J., and Roy, R., *J. Am. Ceram. Soc. C* **5**, 78 (1984).
4. Arsalane, S., Kacimi, M., Ziyad, M., Coudurier, G., and Védrine, J. C., *Appl. Catal. A Gen.* **114**, 243 (1994).

5. Hagman, L. O., and Kierkegaard, P., *Acta Chem. Scand.* **22**, 1822 (1968).
6. Yad, Y. F. Y., and Kummer, J. T., *J. Inorg. Nucl. Chem.* **29**, 2457 (1967).
7. Serghini, A., Kacimi, M., Ziyad, M., and Brochu, R., *J. Chim. Phys.* **85**, 499 (1988).
8. Serghini, A., Thesis, University Mohammed V, Rabat, Morocco, 1991.
9. Monceaux, L., and Courtine, P., *Eur. J. Solid State Inorg. Chem.* **28**,233 (1991).
10. Arsalane, S., Thesis, University Mohammed V, Rabat, Morocco, 1989.
11. Brochu, R., Lamzibri, A., Aadane, A., Arsalane, S., and Ziyad, M., *Eur. J. Solid State Inorg. Chem.* **28**, 253 (1991).
12. Schüth, F., Henry, B. E., and Schmidt, L. D., *Adv. Catal.* **39**, 51 (1993).
13. Arsalane, S., Brochu, R., and Ziyad, M., *C. R. Acad. Sci. Paris,* **311**, 1303 (1990).
14. Jones, A., and McNicol, B. D., "Temperature-Programmed Reduction for Solid Materials Characterization." Dekker, New York, 1986.
15. Dougare, M. K., Singh, P., and Suryavanshi, P. M., *Mater. Res. Bull.* **27**, 637 (1992).
16. El Jazouli, A., Alami, M., Brochu, R., Dance, J. M., Le Flem, G., and Hagenmuller, P., *J. Solid State Chem.* **71**, 444 (1987).
17. Gallens, L. R., Mortier, W. J., Schoonheydt, R. A., and Uytterhoeven, J. B., *J. Phys. Chem.* **85**, 2783 (1981).
18. Oudet, F., Vejux, A., Kompany, T., Bordes, E., and Courtine, P., *Mater. Res. Bull.* **24**, 561 (1989).
19. Chapman, A. C., and Thirlwell, L. E., *Spectrochim. Acta* **20**, 1937 (1964).
20. Cheng, S., and Clearfield, A., *J. Chem. Soc., Faraday Trans. 1* **80**, 1579 (1984).
21. Verykios, X. E., Stein, F. P., and Coughlin, R. W., *J. Catal.* **66**, 368 (1980).
22. Seyedmonir, S. R., Strohmayer, D. E., Guskey, G. J., Geoffoy, G. L., and Vannice, M. A., *J. Catal.* **93**, 288 (1985).
23. Baba, T., Nomura, M., Ono, Y., and Kansaki, Y., *J. Chem. Soc. Faraday Trans.* **88**, 71 (1992).
24. Serghini, A., Brochu, R., Ziyad, M., Loukah, M., and Védrine, J. C., *J. Chem. Soc. Faraday Trans.* **87**, 2487 (1991).
25. Cheng, S., and Clearfield, A., *J. Catal.* **94**, 455 (1985).
26. Kondarides, D. I., and Verykios, X. E., *J. Catal.* **143**, 481 (1993).